UC Berkeley
UC Berkeley Previously Published Works

Title
Observation of B;{0}-->K;(*0)K[over](*0) and Search for B;(0)-->K;(*0)K;(*0).

Permalink
https://escholarship.org/uc/item/18c266hz

Journal
Physical review letters, 100(8)

ISSN
0031-9007

Authors
Aubert, B
Bona, M
Boutigny, D
et al.

Publication Date
2008-02-01

DOI
10.1103/physrevlett.100.081801

Copyright Information
This work is made available under the terms of a Creative Commons Attribution License, availalbe at https://creativecommons.org/licenses/by/4.0/

Peer reviewed

eScholarship.org Powered by the California Digital Library
University of California

Observation of $B^0 \to K^{*0}\bar{K}^{*0}$ and Search for $B^0 \to K^{*0}K^{*0}$

B. Aubert,[1] M. Bona,[1] D. Boutigny,[1] Y. Karyotakis,[1] J. P. Lees,[1] V. Poireau,[1] X. Prudent,[1] V. Tisserand,[1] A. Zghiche,[1] J. Garra Tico,[2] E. Grauges,[2] L. Lopez,[3] A. Palano,[3] M. Pappagallo,[3] G. Eigen,[4] B. Stugu,[4] L. Sun,[4] G. S. Abrams,[5] M. Battaglia,[5] D. N. Brown,[5] J. Button-Shafer,[5] R. N. Cahn,[5] Y. Groysman,[5] R. G. Jacobsen,[5] J. A. Kadyk,[5] L. T. Kerth,[5] Yu. G. Kolomensky,[5] G. Kukartsev,[5] D. Lopes Pegna,[5] G. Lynch,[5] L. M. Mir,[5] T. J. Orimoto,[5] I. L. Osipenkov,[5] M. T. Ronan,[5,*] K. Tackmann,[5] T. Tanabe,[5] W. A. Wenzel,[5] P. del Amo Sanchez,[6] C. M. Hawkes,[6] A. T. Watson,[6] H. Koch,[7] T. Schroeder,[7] D. Walker,[8] D. J. Asgeirsson,[9] T. Cuhadar-Donszelmann,[9] B. G. Fulsom,[9] C. Hearty,[9] T. S. Mattison,[9] J. A. McKenna,[9] A. Khan,[10] M. Saleem,[10] L. Teodorescu,[10] V. E. Blinov,[11] A. D. Bukin,[11] V. P. Druzhinin,[11] V. B. Golubev,[11] A. P. Onuchin,[11] S. I. Serednyakov,[11] Yu. I. Skovpen,[11] E. P. Solodov,[11] K. Yu. Todyshev,[11] M. Bondioli,[12] S. Curry,[12] I. Eschrich,[12] D. Kirkby,[12] A. J. Lankford,[12] P. Lund,[12] M. Mandelkern,[12] E. C. Martin,[12] D. P. Stoker,[12] S. Abachi,[13] C. Buchanan,[13] S. D. Foulkes,[14] J. W. Gary,[14] F. Liu,[14] O. Long,[14] B. C. Shen,[14] G. M. Vitug,[14] L. Zhang,[14] H. P. Paar,[15] S. Rahatlou,[15] V. Sharma,[15] J. W. Berryhill,[16] C. Campagnari,[16] A. Cunha,[16] B. Dahmes,[16] T. M. Hong,[16] D. Kovalskyi,[16] J. D. Richman,[16] T. W. Beck,[17] A. M. Eisner,[17] C. J. Flacco,[17] C. A. Heusch,[17] J. Kroseberg,[17] W. S. Lockman,[17] T. Schalk,[17] B. A. Schumm,[17] A. Seiden,[17] M. G. Wilson,[17] L. O. Winstrom,[17] E. Chen,[18] C. H. Cheng,[18] F. Fang,[18] D. G. Hitlin,[18] I. Narsky,[18] T. Piatenko,[18] F. C. Porter,[18] R. Andreassen,[19] G. Mancinelli,[19] B. T. Meadows,[19] K. Mishra,[19] M. D. Sokoloff,[19] F. Blanc,[20] P. C. Bloom,[20] S. Chen,[20] W. T. Ford,[20] J. F. Hirschauer,[20] A. Kreisel,[20] M. Nagel,[20] U. Nauenberg,[20] A. Olivas,[20] J. G. Smith,[20] K. A. Ulmer,[20] S. R. Wagner,[20] J. Zhang,[20] A. M. Gabareen,[21] A. Soffer,[21,†] W. H. Toki,[21] R. J. Wilson,[21] F. Winklmeier,[21] D. D. Altenburg,[22] E. Feltresi,[22] A. Hauke,[22] H. Jasper,[22] J. Merkel,[22] A. Petzold,[22] B. Spaan,[22] K. Wacker,[22] V. Klose,[23] M. J. Kobel,[23] H. M. Lacker,[23] W. F. Mader,[23] R. Nogowski,[23] J. Schubert,[23] K. R. Schubert,[23] R. Schwierz,[23] J. E. Sundermann,[23] A. Volk,[23] D. Bernard,[24] G. R. Bonneaud,[24] E. Latour,[24] V. Lombardo,[24] Ch. Thiebaux,[24] M. Verderi,[24] P. J. Clark,[25] W. Gradl,[25] F. Muheim,[25] S. Playfer,[25] A. I. Robertson,[25] J. E. Watson,[25] Y. Xie,[25] M. Andreotti,[26] D. Bettoni,[26] C. Bozzi,[26] R. Calabrese,[26] A. Cecchi,[26] G. Cibinetto,[26] P. Franchini,[26] E. Luppi,[26] M. Negrini,[26] A. Petrella,[26] L. Piemontese,[26] E. Prencipe,[26] V. Santoro,[26] F. Anulli,[27] R. Baldini-Ferroli,[27] A. Calcaterra,[27] R. de Sangro,[27] G. Finocchiaro,[27] S. Pacetti,[27] P. Patteri,[27] I. M. Peruzzi,[27] M. Piccolo,[27] M. Rama,[27] A. Zallo,[27] A. Buzzo,[28] R. Contri,[28] M. Lo Vetere,[28] M. M. Macri,[28] M. R. Monge,[28] S. Passaggio,[28] C. Patrignani,[28] E. Robutti,[28] A. Santroni,[28] S. Tosi,[28] K. S. Chaisanguanthum,[29] M. Morii,[29] J. Wu,[29] R. S. Dubitzky,[30] J. Marks,[30] S. Schenk,[30] U. Uwer,[30] D. J. Bard,[31] P. D. Dauncey,[31] R. L. Flack,[31] J. A. Nash,[31] W. Panduro Vazquez,[31] M. Tibbetts,[31] P. K. Behera,[32] X. Chai,[32] M. J. Charles,[32] U. Mallik,[32] J. Cochran,[33] H. B. Crawley,[33] L. Dong,[33] V. Eyges,[33] W. T. Meyer,[33] S. Prell,[33] E. I. Rosenberg,[33] A. E. Rubin,[33] Y. Y. Gao,[34] A. V. Gritsan,[34] Z. J. Guo,[34] C. K. Lae,[34] A. G. Denig,[35] M. Fritsch,[35] G. Schott,[35] N. Arnaud,[36] J. Béquilleux,[36] A. D'Orazio,[36] M. Davier,[36] G. Grosdidier,[36] A. Höcker,[36] V. Lepeltier,[36] F. Le Diberder,[36] A. M. Lutz,[36] S. Pruvot,[36] S. Rodier,[36] P. Roudeau,[36] M. H. Schune,[36] J. Serrano,[36] V. Sordini,[36] A. Stocchi,[36] W. F. Wang,[36] G. Wormser,[36] D. J. Lange,[37] D. M. Wright,[37] I. Bingham,[38] J. P. Burke,[38] C. A. Chavez,[38] J. R. Fry,[38] E. Gabathuler,[38] R. Gamet,[38] D. E. Hutchcroft,[38] D. J. Payne,[38] K. C. Schofield,[38] C. Touramanis,[38] A. J. Bevan,[39] K. A. George,[39] F. Di Lodovico,[39] R. Sacco,[39] G. Cowan,[40] H. U. Flaecher,[40] D. A. Hopkins,[40] S. Paramesvaran,[40] F. Salvatore,[40] A. C. Wren,[40] D. N. Brown,[41] C. L. Davis,[41] J. Allison,[42] D. Bailey,[42] N. R. Barlow,[42] R. J. Barlow,[42] Y. M. Chia,[42] C. L. Edgar,[42] G. D. Lafferty,[42] T. J. West,[42] J. I. Yi,[42] J. Anderson,[43] C. Chen,[43] A. Jawahery,[43] D. A. Roberts,[43] G. Simi,[43] J. M. Tuggle,[43] G. Blaylock,[44] C. Dallapiccola,[44] S. S. Hertzbach,[44] X. Li,[44] T. B. Moore,[44] E. Salvati,[44] S. Saremi,[44] R. Cowan,[45] D. Dujmic,[45] P. H. Fisher,[45] K. Koeneke,[45] G. Sciolla,[45] M. Spitznagel,[45] F. Taylor,[45] R. K. Yamamoto,[45] M. Zhao,[45] Y. Zheng,[45] S. E. Mclachlin,[46,*] P. M. Patel,[46] S. H. Robertson,[46] A. Lazzaro,[47] F. Palombo,[47] J. M. Bauer,[48] L. Cremaldi,[48] V. Eschenburg,[48] R. Godang,[48] R. Kroeger,[48] D. A. Sanders,[48] D. J. Summers,[48] H. W. Zhao,[48] S. Brunet,[49] D. Côté,[49] M. Simard,[49] P. Taras,[49] F. B. Viaud,[49] H. Nicholson,[50] G. De Nardo,[51] F. Fabozzi,[51,§] L. Lista,[51] D. Monorchio,[51] C. Sciacca,[51] M. A. Baak,[52] G. Raven,[52] H. L. Snoek,[52] C. P. Jessop,[53] K. J. Knoepfel,[53] J. M. LoSecco,[53] G. Benelli,[54] L. A. Corwin,[54] K. Honscheid,[54] H. Kagan,[54] R. Kass,[54] J. P. Morris,[54] A. M. Rahimi,[54] J. J. Regensburger,[54] S. J. Sekula,[54] Q. K. Wong,[54] N. L. Blount,[55] J. Brau,[55] R. Frey,[55] O. Igonkina,[55] J. A. Kolb,[55] M. Lu,[55] R. Rahmat,[55] N. B. Sinev,[55] D. Strom,[55] J. Strube,[55] E. Torrence,[55] N. Gagliardi,[56] A. Gaz,[56] M. Margoni,[56] M. Morandin,[56] A. Pompili,[56] M. Posocco,[56] M. Rotondo,[56] F. Simonetto,[56] R. Stroili,[56] C. Voci,[56] E. Ben-Haim,[57] H. Briand,[57] G. Calderini,[57] J. Chauveau,[57] P. David,[57] L. Del Buono,[57] Ch. de la Vaissière,[57] O. Hamon,[57] Ph. Leruste,[57] J. Malclès,[57] J. Ocariz,[57] A. Perez,[57] J. Prendki,[57] L. Gladney,[58] M. Biasini,[59] R. Covarelli,[59] E. Manoni,[59] C. Angelini,[60] G. Batignani,[60]

 © 2008 The American Physical Society

S. Bettarini,[60] M. Carpinelli,[60] R. Cenci,[60] A. Cervelli,[60] F. Forti,[60] M. A. Giorgi,[60] A. Lusiani,[60] G. Marchiori,[60] M. A. Mazur,[60] M. Morganti,[60] N. Neri,[60] E. Paoloni,[60] G. Rizzo,[60] J. J. Walsh,[60] J. Biesiada,[61] P. Elmer,[61] Y. P. Lau,[61] C. Lu,[61] J. Olsen,[61] A. J. S. Smith,[61] A. V. Telnov,[61] E. Baracchini,[62] F. Bellini,[62] G. Cavoto,[62] D. del Re,[62] E. Di Marco,[62] R. Faccini,[62] F. Ferrarotto,[62] F. Ferroni,[62] M. Gaspero,[62] P. D. Jackson,[62] L. Li Gioi,[62] M. A. Mazzoni,[62] S. Morganti,[62] G. Piredda,[62] F. Polci,[62] F. Renga,[62] C. Voena,[62] M. Ebert,[63] T. Hartmann,[63] H. Schröder,[63] R. Waldi,[63] T. Adye,[64] G. Castelli,[64] B. Franek,[64] E. O. Olaiya,[64] W. Roethel,[64] F. F. Wilson,[64] S. Emery,[65] M. Escalier,[65] A. Gaidot,[65] S. F. Ganzhur,[65] G. Hamel de Monchenault,[65] W. Kozanecki,[65] G. Vasseur,[65] Ch. Yèche,[65] M. Zito,[65] X. R. Chen,[66] H. Liu,[66] W. Park,[66] M. V. Purohit,[66] R. M. White,[66] J. R. Wilson,[66] M. T. Allen,[67] D. Aston,[67] R. Bartoldus,[67] P. Bechtle,[67] R. Claus,[67] J. P. Coleman,[67] M. R. Convery,[67] J. C. Dingfelder,[67] J. Dorfan,[67] G. P. Dubois-Felsmann,[67] W. Dunwoodie,[67] R. C. Field,[67] T. Glanzman,[67] S. J. Gowdy,[67] M. T. Graham,[67] P. Grenier,[67] C. Hast,[67] W. R. Innes,[67] J. Kaminski,[67] M. H. Kelsey,[67] H. Kim,[67] P. Kim,[67] M. L. Kocian,[67] D. W. G. S. Leith,[67] S. Li,[67] S. Luitz,[67] V. Luth,[67] H. L. Lynch,[67] D. B. MacFarlane,[67] H. Marsiske,[67] R. Messner,[67] D. R. Muller,[67] C. P. O'Grady,[67] I. Ofte,[67] A. Perazzo,[67] M. Perl,[67] T. Pulliam,[67] B. N. Ratcliff,[67] A. Roodman,[67] A. A. Salnikov,[67] R. H. Schindler,[67] J. Schwiening,[67] A. Snyder,[67] D. Su,[67] M. K. Sullivan,[67] K. Suzuki,[67] S. K. Swain,[67] J. M. Thompson,[67] J. Va'vra,[67] A. P. Wagner,[67] M. Weaver,[67] W. J. Wisniewski,[67] M. Wittgen,[67] D. H. Wright,[67] A. K. Yarritu,[67] K. Yi,[67] C. C. Young,[67] V. Ziegler,[67] P. R. Burchat,[68] A. J. Edwards,[68] S. A. Majewski,[68] T. S. Miyashita,[68] B. A. Petersen,[68] L. Wilden,[68] S. Ahmed,[69] M. S. Alam,[69] R. Bula,[69] J. A. Ernst,[69] V. Jain,[69] B. Pan,[69] M. A. Saeed,[69] F. R. Wappler,[69] S. B. Zain,[69] M. Krishnamurthy,[70] S. M. Spanier,[70] R. Eckmann,[71] J. L. Ritchie,[71] A. M. Ruland,[71] C. J. Schilling,[71] R. F. Schwitters,[71] J. M. Izen,[72] X. C. Lou,[72] S. Ye,[72] F. Bianchi,[73] F. Gallo,[73] D. Gamba,[73] M. Pelliccioni,[73] M. Bomben,[74] L. Bosisio,[74] C. Cartaro,[74] F. Cossutti,[74] G. Della Ricca,[74] L. Lanceri,[74] L. Vitale,[74] V. Azzolini,[75] N. Lopez-March,[75] F. Martinez-Vidal,[75,‖] D. A. Milanes,[75] A. Oyanguren,[75] J. Albert,[76] Sw. Banerjee,[76] B. Bhuyan,[76] K. Hamano,[76] R. Kowalewski,[76] I. M. Nugent,[76] J. M. Roney,[76] R. J. Sobie,[76] P. F. Harrison,[77] J. Ilic,[77] T. E. Latham,[77] G. B. Mohanty,[77] H. R. Band,[78] X. Chen,[78] S. Dasu,[78] K. T. Flood,[78] J. J. Hollar,[78] P. E. Kutter,[78] Y. Pan,[78] M. Pierini,[78] R. Prepost,[78] S. L. Wu,[78] and H. Neal[79]

(*BABAR* Collaboration)

[1]*Laboratoire de Physique des Particules, IN2P3/CNRS et Université de Savoie, F-74941 Annecy-Le-Vieux, France*
[2]*Universitat de Barcelona, Facultat de Fisica, Departament ECM, E-08028 Barcelona, Spain*
[3]*Università di Bari, Dipartimento di Fisica and INFN, I-70126 Bari, Italy*
[4]*University of Bergen, Institute of Physics, N-5007 Bergen, Norway*
[5]*Lawrence Berkeley National Laboratory and University of California, Berkeley, California 94720, USA*
[6]*University of Birmingham, Birmingham B15 2TT, United Kingdom*
[7]*Ruhr Universität Bochum, Institut für Experimentalphysik 1, D-44780 Bochum, Germany*
[8]*University of Bristol, Bristol BS8 1TL, United Kingdom*
[9]*University of British Columbia, Vancouver, British Columbia, Canada V6T 1Z1*
[10]*Brunel University, Uxbridge, Middlesex UB8 3PH, United Kingdom*
[11]*Budker Institute of Nuclear Physics, Novosibirsk 630090, Russia*
[12]*University of California at Irvine, Irvine, California 92697, USA*
[13]*University of California at Los Angeles, Los Angeles, California 90024, USA*
[14]*University of California at Riverside, Riverside, California 92521, USA*
[15]*University of California at San Diego, La Jolla, California 92093, USA*
[16]*University of California at Santa Barbara, Santa Barbara, California 93106, USA*
[17]*University of California at Santa Cruz, Institute for Particle Physics, Santa Cruz, California 95064, USA*
[18]*California Institute of Technology, Pasadena, California 91125, USA*
[19]*University of Cincinnati, Cincinnati, Ohio 45221, USA*
[20]*University of Colorado, Boulder, Colorado 80309, USA*
[21]*Colorado State University, Fort Collins, Colorado 80523, USA*
[22]*Universität Dortmund, Institut für Physik, D-44221 Dortmund, Germany*
[23]*Technische Universität Dresden, Institut für Kern- und Teilchenphysik, D-01062 Dresden, Germany*
[24]*Laboratoire Leprince-Ringuet, CNRS/IN2P3, Ecole Polytechnique, F-91128 Palaiseau, France*
[25]*University of Edinburgh, Edinburgh EH9 3JZ, United Kingdom*
[26]*Università di Ferrara, Dipartimento di Fisica and INFN, I-44100 Ferrara, Italy*
[27]*Laboratori Nazionali di Frascati dell'INFN, I-00044 Frascati, Italy*
[28]*Università di Genova, Dipartimento di Fisica and INFN, I-16146 Genova, Italy*
[29]*Harvard University, Cambridge, Massachusetts 02138, USA*
[30]*Universität Heidelberg, Physikalisches Institut, Philosophenweg 12, D-69120 Heidelberg, Germany*

[31]*Imperial College London, London SW7 2AZ, United Kingdom*
[32]*University of Iowa, Iowa City, Iowa 52242, USA*
[33]*Iowa State University, Ames, Iowa 50011-3160, USA*
[34]*Johns Hopkins University, Baltimore, Maryland 21218, USA*
[35]*Universität Karlsruhe, Institut für Experimentelle Kernphysik, D-76021 Karlsruhe, Germany*
[36]*Laboratoire de l'Accélérateur Linéaire, IN2P3/CNRS et Université Paris-Sud 11, Centre Scientifique d'Orsay, B. P. 34, F-91898 ORSAY Cedex, France*
[37]*Lawrence Livermore National Laboratory, Livermore, California 94550, USA*
[38]*University of Liverpool, Liverpool L69 7ZE, United Kingdom*
[39]*Queen Mary, University of London, E1 4NS, United Kingdom*
[40]*University of London, Royal Holloway and Bedford New College, Egham, Surrey TW20 0EX, United Kingdom*
[41]*University of Louisville, Louisville, Kentucky 40292, USA*
[42]*University of Manchester, Manchester M13 9PL, United Kingdom*
[43]*University of Maryland, College Park, Maryland 20742, USA*
[44]*University of Massachusetts, Amherst, Massachusetts 01003, USA*
[45]*Massachusetts Institute of Technology, Laboratory for Nuclear Science, Cambridge, Massachusetts 02139, USA*
[46]*McGill University, Montréal, Québec, Canada H3A 2T8*
[47]*Università di Milano, Dipartimento di Fisica and INFN, I-20133 Milano, Italy*
[48]*University of Mississippi, University, Mississippi 38677, USA*
[49]*Université de Montréal, Physique des Particules, Montréal, Québec, Canada H3C 3J7*
[50]*Mount Holyoke College, South Hadley, Massachusetts 01075, USA*
[51]*Università di Napoli Federico II, Dipartimento di Scienze Fisiche and INFN, I-80126, Napoli, Italy*
[52]*NIKHEF, National Institute for Nuclear Physics and High Energy Physics, NL-1009 DB Amsterdam, The Netherlands*
[53]*University of Notre Dame, Notre Dame, Indiana 46556, USA*
[54]*The Ohio State University, Columbus, Ohio 43210, USA*
[55]*University of Oregon, Eugene, Oregon 97403, USA*
[56]*Università di Padova, Dipartimento di Fisica and INFN, I-35131 Padova, Italy*
[57]*Laboratoire de Physique Nucléaire et de Hautes Energies, IN2P3/CNRS, Université Pierre et Marie Curie-Paris 6, Université Denis Diderot-Paris 7, F-75252 Paris, France*
[58]*University of Pennsylvania, Philadelphia, Pennsylvania 19104, USA*
[59]*Università di Perugia, Dipartimento di Fisica and INFN, I-06100 Perugia, Italy*
[60]*Università di Pisa, Dipartimento di Fisica, Scuola Normale Superiore and INFN, I-56127 Pisa, Italy*
[61]*Princeton University, Princeton, New Jersey 08544, USA*
[62]*Università di Roma La Sapienza, Dipartimento di Fisica and INFN, I-00185 Roma, Italy*
[63]*Universität Rostock, D-18051 Rostock, Germany*
[64]*Rutherford Appleton Laboratory, Chilton, Didcot, Oxon OX11 0QX, United Kingdom*
[65]*DSM/Dapnia, CEA/Saclay, F-91191 Gif-sur-Yvette, France*
[66]*University of South Carolina, Columbia, South Carolina 29208, USA*
[67]*Stanford Linear Accelerator Center, Stanford, California 94309, USA*
[68]*Stanford University, Stanford, California 94305-4060, USA*
[69]*State University of New York, Albany, New York 12222, USA*
[70]*University of Tennessee, Knoxville, Tennessee 37996, USA*
[71]*University of Texas at Austin, Austin, Texas 78712, USA*
[72]*University of Texas at Dallas, Richardson, Texas 75083, USA*
[73]*Università di Torino, Dipartimento di Fisica Sperimentale and INFN, I-10125 Torino, Italy*
[74]*Università di Trieste, Dipartimento di Fisica and INFN, I-34127 Trieste, Italy*
[75]*IFIC, Universitat de Valencia-CSIC, E-46071 Valencia, Spain*
[76]*University of Victoria, Victoria, British Columbia, Canada V8W 3P6*
[77]*Department of Physics, University of Warwick, Coventry CV4 7AL, United Kingdom*
[78]*University of Wisconsin, Madison, Wisconsin 53706, USA*
[79]*Yale University, New Haven, Connecticut 06511, USA*

(Received 16 August 2007; published 25 February 2008)

We report the observation of the $b \to d$ penguin-dominated decay $B^0 \to K^{*0}\bar{K}^{*0}$ with a sample of 383.2 ± 4.2 million $B\bar{B}$ pairs collected with the *BABAR* detector at the PEP-II asymmetric-energy e^+e^- collider at the Stanford Linear Accelerator Center. The measured branching fraction is $\mathcal{B}(B^0 \to K^{*0}\bar{K}^{*0}) = [1.28^{+0.35}_{-0.30} \pm 0.11] \times 10^{-6}$ and the fraction of longitudinal polarization is $f_L(B^0 \to K^{*0}\bar{K}^{*0}) = 0.80^{+0.10}_{-0.12} \pm 0.06$. The first error quoted is statistical and the second systematic. We also obtain an upper limit at the 90% confidence level on the branching fraction for $\mathcal{B}(B^0 \to K^{*0}K^{*0}) < 0.41 \times 10^{-6}$.

DOI: 10.1103/PhysRevLett.100.081801 PACS numbers: 13.25.Hw, 11.30.Er, 12.15.Hh

The study of the branching fractions and angular distributions of B meson decays to hadronic final states without a charm quark probes the dynamics of both weak and strong interactions, and plays an important role in understanding CP violation. Decays proceeding via electroweak and gluonic $b \to d$ penguin diagrams have only recently been measured in the decays $B \to \rho\gamma$ [1] and $B^0 \to K^0\bar{K}^0$ [2]. On the other hand, the charmless decay $B^0 \to K^{*0}\bar{K}^{*0}$ proceeds through both electroweak and gluonic $b \to d$ penguin loops to two vector particles (VV). The standard model (SM) suppressed decay $B^0 \to K^{*0}K^{*0}$ could appear via an intermediate heavy boson.

Theoretical models in the framework of QCD factorization predict the angular distribution of the VV decays of the B meson, as measured by the longitudinal polarization fraction f_L, to be $\sim$0.9 for both tree- and penguin-dominated decays [3]. However, recent measurements of the pure penguin VV decay $B \to \phi K^*$ indicate $f_L \sim 0.5$ [4]. Several attempts to understand this unexpected value of f_L within or beyond the standard model have been made [5]. Further information about decays related by $SU(3)$ symmetry may provide insight into this polarization puzzle and test factorization models. A time-dependent angular analysis of $B^0 \to K^{*0}\bar{K}^{*0}$ can distinguish between penguin annihilation and rescattering as mechanisms for the value of f_L observed in $B \to \phi K^*$ [6]. The $B^0 \to K^{*0}\bar{K}^{*0}$ mode can also be used within the SM framework to help constrain the angles α and γ of the unitarity triangle [7].

Theoretical calculations for $B^0 \to K^{*0}\bar{K}^{*0}$ branching fractions cover the range $(0.16\text{–}0.96) \times 10^{-6}$ [8]. Recently, Beneke, Rohrer, and Yang [9] predicted $(0.6^{+0.1+0.3}_{-0.1-0.2}) \times 10^{-6}$ and $f_L = 0.69 \pm 0.01^{+0.16}_{-0.20}$. Experimentally, upper limits on the branching fractions at the 90% confidence level (CL) of 22×10^{-6} and 37×10^{-6} exist for $B^0 \to K^{*0}\bar{K}^{*0}$ and $B^0 \to K^{*0}K^{*0}$, respectively [10].

We report measurements of the branching fraction and the fraction of longitudinal polarization for the decay mode $B^0 \to K^{*0}\bar{K}^{*0}$, with explicit consideration of nonresonant backgrounds and interference from $K^{*0}\bar{K}^{*0}(1430)$. We place an upper limit on the branching fraction of $B^0 \to K^{*0}K^{*0}$, where we use the notation $K^{*0}K^{*0}$ to also represent $\bar{K}^{*0}\bar{K}^{*0}$. Charge-conjugate modes are implied throughout, and we assume equal production rates of B^+B^- and $B^0\bar{B}^0$.

This analysis is based on a data sample of 383.2 ± 4.2 million $B\bar{B}$ pairs, corresponding to an integrated luminosity of 348 fb^{-1}, collected with the *BABAR* detector at the PEP-II asymmetric-energy e^+e^- collider operated at the Stanford Linear Accelerator Center. The e^+e^- center-of-mass (c.m.) energy is $\sqrt{s} = 10.58$ GeV, corresponding to the $\Upsilon(4S)$ resonance mass (on-resonance data). In addition, 36.6 fb^{-1} of data collected 40 MeV below the $\Upsilon(4S)$ resonance (off-resonance data) are used for background studies.

The *BABAR* detector is described in detail in Ref. [11]. Charged particles are reconstructed as tracks with a 5-layer silicon vertex detector and a 40-layer drift chamber inside a 1.5-T solenoidal magnet. An electromagnetic calorimeter is used to identify electrons and photons. A ring-imaging Cherenkov detector is used to identify charged hadrons and provides additional electron identification information. Muons are identified by an instrumented magnetic-flux return.

The $B^0 \to K^{*0}\bar{K}^{*0}$ and $B^0 \to K^{*0}K^{*0}$ candidates are reconstructed through the decays $K^{*0} \to K^+\pi^-$ and $\bar{K}^{*0} \to K^-\pi^+$. The differential decay rate, after integrating over the angle between the decay planes of the vector mesons, for which the acceptance is uniform, is

$$\frac{1}{\Gamma}\frac{d^2\Gamma}{d\cos\theta_1 d\cos\theta_2} \propto \frac{1-f_L}{4}\sin^2\theta_1\sin^2\theta_2 + f_L\cos^2\theta_1\cos^2\theta_2, \tag{1}$$

where θ_1 and θ_2 are the helicity angles of the K^{*0} or $\bar{K}^{*0}$. The helicity angle of the $K^{*0}(\bar{K}^{*0})$ is defined as the angle between the $K^+(K^-)$ momentum and the direction opposite to the B meson in the $K^{*0}(\bar{K}^{*0})$ rest frame [12].

The charged tracks from the K^{*0} decays are required to have at least 12 hits in the drift chamber and a transverse momentum greater than 0.1 GeV/c. The tracks are identified as either pions or kaons by measurement of the energy loss in the tracking devices, the number of photons measured by the Cherenkov detector, and the corresponding Cherenkov angles. These measurements are combined with calorimeter information to reject electrons, muons, and protons. We require the invariant mass of the K^{*0} candidates to be $0.792 < m_{K\pi} < 1.025$ GeV/c^2. A B meson candidate is formed from two K^{*0} candidates, with the constraint that the two K^{*0} candidates originate from the interaction region.

B meson candidates are characterized kinematically by the energy difference $\Delta E = E_B^* - \sqrt{s}/2$ and the energy-substituted mass $m_{\rm ES} = [(s/2 + \mathbf{p}_i \cdot \mathbf{p}_B)^2/E_i^2 - \mathbf{p}_B^2]^{1/2}$, where $(E_i, \mathbf{p}_i)$ and $(E_B, \mathbf{p}_B)$ are the four-momenta of the $\Upsilon(4S)$ and B meson candidate, respectively, and the asterisk denotes the $\Upsilon(4S)$ rest frame. The total event sample is taken from the region $-0.08 \le \Delta E \le 0.2$ GeV and $5.25 \le m_{\rm ES} \le 5.29$ GeV/c^2. Events outside the region $|\Delta E| \le 0.07$ GeV and $5.27 \le m_{\rm ES} \le 5.29$ GeV/c^2 are used to characterize the background. The average number of signal B meson candidates per selected data event is 1.03. A single B meson candidate per event is chosen as the one whose fitted decay vertex has the smallest χ^2. Monte Carlo (MC) simulations show that up to 4% (1.6%) of longitudinally (transversely) polarized signal events are misreconstructed, with one or more tracks originating from the other B meson in the event.

To reject the dominant background consisting of light-quark $q\bar{q}$ ($q = u, d, s, c$) continuum events, we require $|\cos\theta_T| < 0.8$, where θ_T is the angle, in the c.m. frame, between the thrust axes [13] of the B meson and that formed from the other tracks and neutral clusters in the event. We create a Fisher discriminant $\mathcal{F}$ to be used in the maximum-likelihood (ML) fit, constructed from a linear combination of five variables: the polar angles of the B meson momentum vector and the B meson thrust axis with respect to the beam axis, the ratio of the second- and zeroth-order momentum-weighted Legendre polynomial moments of the energy flow around the B meson thrust axis in the c.m. frame [14], the flavor of the other B meson as reported by a multivariate tagging algorithm [15], and the boost-corrected proper-time difference between the decays of the two B mesons divided by its variance. The second B meson is formed by creating a vertex from the remaining tracks that are consistent with originating from the interaction region.

We suppress background from decays to charmed states by removing candidates that have decays consistent with $D^- \to K^+\pi^-\pi^-$ and an invariant mass in the range $1.845 < m_{K^+\pi^-\pi^-} < 1.895$ GeV$/c^2$. We reduce backgrounds from $B^0 \to \phi K^{*0}$ by assigning the kaon mass to the pion candidate and rejecting the event if the combined invariant mass of the two charged tracks is between 1.00 and 1.04 GeV$/c^2$. Finally, we require the cosine of the helicity angle of both K^{*0} candidates to be less than 0.98 to reduce the continuum background and avoid the region where the reconstruction efficiency falls off rapidly.

We use an extended unbinned ML fit to extract the signal yield and polarization simultaneously for each mode. The extended likelihood function is

$$\mathcal{L} = \frac{1}{N!}\exp\left(-\sum_j n_j\right)\prod_{i=1}^{N}\left[\sum_j n_j \mathcal{P}_j(\vec{x}_i;\vec{\alpha}_j)\right]. \quad (2)$$

We define the likelihood $\mathcal{L}_i$ for each event candidate i as the sum of $n_j\mathcal{P}_j(\vec{x}_i;\vec{\alpha}_j)$ over four hypotheses j (signal, $q\bar{q}$ background, $K^{*0}(1430)$ and $B\bar{B}$ backgrounds as discussed below), where $\mathcal{P}_j(\vec{x}_i;\vec{\alpha}_j)$ is the product of the probability density functions (PDFs) for hypothesis j evaluated for the ith event's measured variables $\vec{x}_i$, n_j is the yield for hypothesis j, and N is the total number of events in the sample. The quantities $\vec{\alpha}_j$ represent parameters in the expected distributions of the measured variables for each hypothesis j. Each discriminating variable $\vec{x}_i$ in the likelihood function is modeled with a PDF, where the parameters $\vec{\alpha}_j$ are extracted from MC simulation, off-resonance data, or ($m_{\rm ES}$, ΔE) sideband data.

The seven variables $\vec{x}_i$ used in the fit are $m_{\rm ES}$, ΔE, $\mathcal{F}$, and the invariant masses and cosines of the helicity angle of the two K^{*0} candidates. Since the correlations among the fitted input variables are found to be on average $\sim$1% with a maximum of 4%, we take each $\mathcal{P}_j$ to be the product of the PDFs for the separate variables. The effect of neglecting correlations is evaluated by fitting ensembles of simulated experiments in which we embed signal and background events randomly extracted from fully simulated MC samples.

The two invariant mass and helicity angle distributions for each K^{*0} meson are indistinguishable, and so we use the same PDF parameters for both K^{*0} candidates. Peaking PDF distributions are described with an asymmetric Gaussian or a sum of two Gaussians. The transverse (longitudinal) helicity angle distributions are described with a $\cos^2\theta$ ($\sin^2\theta$) function corrected for changes in efficiency as a function of helicity angle. The $B\bar{B}$ backgrounds use an empirical nonparametric function for ΔE, the masses, and helicity angles. The continuum background $m_{\rm ES}$ shape is described by the function $x\sqrt{1-x^2}\exp[-\xi(1-x^2)]$ (with $x = m_{\rm ES}/E_B^*$ and ξ a free parameter) [16], and a first- or third-order polynomial is used for ΔE and the helicity angles, respectively. The continuum invariant mass distributions contain real K^{*0} candidates; we model the peaking mass component using the parameters extracted from the fit to the signal invariant mass distributions together with a second-order polynomial to represent the nonpeaking component.

We use the decay $B^0 \to D^-\pi^+ (D^- \to K^{*0}\pi^-)$ as a calibration channel to account for small differences between MC simulation and reconstructed data. This decay has a similar topology to the modes under study and is selected using the same criteria as for $K^{*0}\bar{K}^{*0}$ but requiring the reconstructed $K^{*0}\pi^{\pm}$ invariant mass to be in the range $1.845 < m_{K^{*0}\pi^{\pm}} < 1.895$ GeV$/c^2$. We predict 1860 ± 186 signal events and measure 1614 ± 47.

We use MC-simulated events to study backgrounds from other B meson decays. The major charmless $B\bar{B}$ background to $B^0 \to K^{*0}\bar{K}^{*0}$ is $B^0 \to \phi K^{*0}$, while charm $B\bar{B}$ backgrounds are effectively suppressed by the requirement that the two pions (and kaons) have opposite charge. For $B^0 \to K^{*0}K^{*0}$, $B^0 \to \phi K^{*0}$ remains the major charmless $B\bar{B}$ background, but a number of charm decays contaminate the signal, dominated by decays of the type $B^0 \to D^-K^+$ and $B^- \to D^0K^-$. Given the uncertainty in the polarization and branching fractions of these backgrounds, we allow the $B\bar{B}$ background yield to float in the fit.

A possible background is the decay $B^0 \to K^{*0}\bar{K}^{*0}(1430)$. We use the LASS parametrization for the $\bar{K}^{*0}(1430)$ line shape, which consists of the $\bar{K}^{*0}(1430)$ resonance together with an effective-range nonresonant component [17]. We apply the same selection criteria used for $K^{*0}\bar{K}^{*0}$ but require one of the K^{*0} candidates to have an invariant mass in the range $1.025 < m_{K\pi} < 1.53$ GeV$/c^2$ and perform an extended unbinned ML fit with the four variables $m_{\rm ES}$, ΔE, $\mathcal{F}$, and the K^{*0} mass. We fit the LASS parametrization to the selected signal events

TABLE I. Summary of results: signal yield n_{sig}, the $B\bar{B}$ background yield $n_{B\bar{B}}$, signal reconstruction efficiency ε [taking into account that $\mathcal{B}(K^{*0} \to K^+\pi^-) = 2/3$], significance S (systematic uncertainties included), branching fraction $\mathcal{B}$, 90% CL upper limit for $B^0 \to K^{*0}K^{*0}$ branching fraction, and the longitudinal polarization f_L. The first error given is statistical and the second is systematic.

Channel	$K^{*0}\bar{K}^{*0}$	$K^{*0}K^{*0}$
n_{sig}	$33.5^{+9.1}_{-8.1}$	2.7 ± 3.3
$n_{B\bar{B}}$	19 ± 12	68 ± 29
ε (%)	6.8	6.4
$S(\sigma)$	6	0.9
$\mathcal{B}(10^{-6})$	$1.28^{+0.35}_{-0.30} \pm 0.11$	$0.11^{+0.16}_{-0.11} \pm 0.04$
UL $\mathcal{B}(10^{-6})$	$\cdots$	0.41
f_L	$0.80^{+0.10}_{-0.12} \pm 0.06$	1.0 ± 1.0

in the $\bar{K}^{*0}(1430)$ mass range and extrapolate to the K^{*0} mass range. Interference effects between the K^{*0} and the spin-0 final states [nonresonant and $\bar{K}^{*0}(1430)$] integrate to zero as the acceptance of the detector and analysis is uniform. Assuming no interference, we expect 6 ± 5 $B^0 \to K^{*0}\bar{K}^{*0}(1430)$ events in the fitted $B^0 \to K^{*0}\bar{K}^{*0}$ signal region. The uncertainty on the contribution is calculated from the statistical error and the large uncertainty in the fitted LASS parameters used to describe the $\bar{K}^{*0}(1430)$ line shape. We fix the yield in the final fit and vary the yield by its error to assess the systematic uncertainty.

The continuum background PDF parameters that are allowed to vary are the $\mathcal{F}$ peak position, ξ for m_{ES}, the slope of ΔE, and the polynomial coefficients and normalization describing the mass and helicity angle distributions. We fit for $\mathcal{B}$ and f_L directly and exploit the fact that $\mathcal{B}$ is less correlated with f_L than is either the yield or the efficiency taken separately.

The total event sample consists of 7363 and 1390 events for $B^0 \to K^{*0}\bar{K}^{*0}$ and $B^0 \to K^{*0}K^{*0}$, respectively. The results of the ML fits are summarized in Table I. The $B\bar{B}$ background yield agrees with the MC prediction within the statistical errors. The significance S of the signal is defined as $S = 2\Delta\ln\mathcal{L}$, where $\Delta\ln\mathcal{L}$ is the change in likelihood from the maximum value when the number of signal events is set to zero, corrected for the systematic error defined below. The robustness of the significance estimate is cross-checked through fitting a series of toy MC ensembles generated from the fitted parameters. The significance of the $B^0 \to K^{*0}\bar{K}^{*0}$ branching fraction is 6σ, including statistical and systematic uncertainties. For $B^0 \to K^{*0}K^{*0}$, we compute the 90% CL upper limit as the branching fraction below which lies 90% of the total likelihood integral, taking into account the systematic uncertainty. Figure 1 shows the projections of the fits onto m_{ES}, ΔE, K^{*0} mass and cosine of the K^{*0} helicity angle for $B^0 \to K^{*0}\bar{K}^{*0}$.

Systematic uncertainties in the branching fractions are dominated by our knowledge of the PDF modeling. Varying the PDF parameters by their errors results in changes in the yields of 6.5% and 19.0% for $B^0 \to K^{*0}\bar{K}^{*0}$ and $B^0 \to K^{*0}K^{*0}$, respectively. The largest contribution comes from the width of the K^{*0}.

The reconstruction efficiency depends on the decay polarization. We calculate the efficiency using the measured polarization and assign a systematic error from the

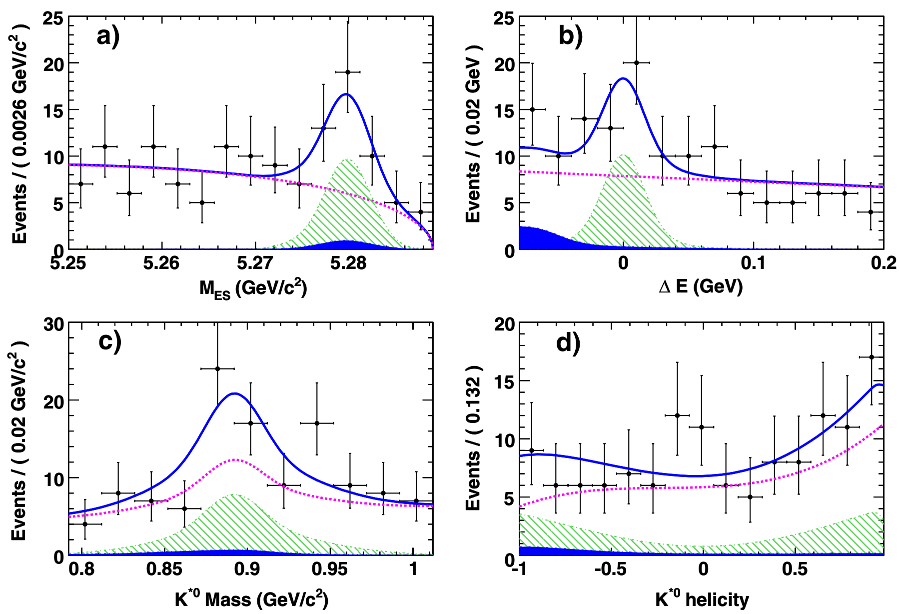

FIG. 1 (color online). Projections of the multidimensional fit onto (a) m_{ES}; (b) ΔE; (c) K^{*0} mass; and (d) cosine of K^{*0} helicity angle for $B^0 \to K^{*0}\bar{K}^{*0}$ events selected with a requirement on the signal-to-total likelihood probability ratio, optimized for each variable, with the plotted variable excluded. The points with error bars show the data; the solid line shows signal-plus-background; the dashed line is the continuum background; the hatched region is the signal; and the shaded region is the $B\bar{B}$ background.

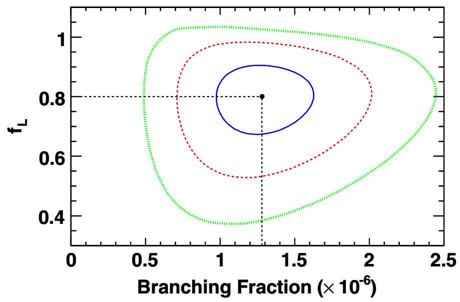

FIG. 2 (color online). Distribution of $-2\ln\mathcal{L}(\mathcal{B}, f_L)$ for $B^0 \to K^{*0}\bar{K}^{*0}$ decays. The solid dot shows the central value and the curves give contours in steps of one sigma $[\Delta\sqrt{-2\ln\mathcal{L}(\mathcal{B}, f_L)} = 1]$.

uncertainty on f_L of 3.4% and 27.0% for $B^0 \to K^{*0}\bar{K}^{*0}$ and $B^0 \to K^{*0}K^{*0}$, respectively. Figure 2 shows the behavior of $-2\ln\mathcal{L}(\mathcal{B}, f_L)$ for the $B^0 \to K^{*0}\bar{K}^{*0}$ mode.

The uncertainties in PDF modeling and f_L are additive in nature and affect the significance of the branching fraction results. Multiplicative uncertainties include reconstruction efficiency uncertainties from tracking (3.2%) and particle identification (4.4%), track multiplicity (1%), MC signal efficiency statistics (0.6%), and the number of $B\bar{B}$ pairs (1.1%). Variation of the expected yield from $B^0 \to K^{*0}\bar{K}^{*0}(1430)$ events has a negligible effect on the signal.

The systematic uncertainty in f_L is dominated by the PDF shape variations, which contribute 7% for $B^0 \to K^{*0}\bar{K}^{*0}$ and 20% for $B^0 \to K^{*0}K^{*0}$. Other errors identified above for the branching fraction have a very small effect on f_L and contribute in total 0.7%. The total systematic error is summarized in Table I.

In summary, we have measured the branching fraction $\mathcal{B}(B^0 \to K^{*0}\bar{K}^{*0}) = [1.28^{+0.35}_{-0.30}(\text{stat}) \pm 0.11(\text{syst})] \times 10^{-6}$ with a significance of 6σ. We find the fraction of longitudinal polarization $f_L = 0.80^{+0.10}_{-0.12}(\text{stat}) \pm 0.06(\text{syst})$. Both results are in agreement with the upper range of theoretical predictions. The 90% CL upper limit on the branching fraction $\mathcal{B}(B^0 \to K^{*0}K^{*0}) < 0.41 \times 10^{-6}$ is 2 orders of magnitude more stringent than previous measurements.

We are grateful for the excellent luminosity and machine conditions provided by our PEP-II colleagues, and for the substantial dedicated effort from the computing organizations that support *BABAR*. The collaborating institutions wish to thank SLAC for its support and kind hospitality. This work is supported by DOE and NSF (USA), NSERC (Canada), CEA and CNRS-IN2P3 (France), BMBF and DFG (Germany), INFN (Italy), FOM (The Netherlands), NFR (Norway), MIST (Russia), MEC (Spain), and STFC (United Kingdom). Individuals have received support from the Marie Curie Actions (European Union) and the A. P. Sloan Foundation.

*Deceased.
†Present address: Tel Aviv University, Tel Aviv, 69978, Israel.
‡Also at Università di Perugia, Dipartimento di Fisica, Perugia, Italy.
§Also at Università della Basilicata, Potenza, Italy.
‖Also at Universitat de Barcelona, Facultat de Fisica, Departament ECM, E-08028 Barcelona, Spain.

[1] B. Aubert *et al.* (*BABAR* Collaboration), Phys. Rev. Lett. **98**, 151802 (2007); D. Mohapatra *et al.* (Belle Collaboration), Phys. Rev. Lett. **96**, 221601 (2006).
[2] B. Aubert *et al.* (*BABAR* Collaboration), Phys. Rev. Lett. **97**, 171805 (2006); S.-W. Lin *et al.* (Belle Collaboration), Phys. Rev. Lett. **98**, 181804 (2007).
[3] A. Ali *et al.*, Z. Phys. C **1**, 269 (1979); M. Suzuki, Phys. Rev. D **66**, 054018 (2002).
[4] B. Aubert *et al.* (*BABAR* Collaboration), Phys. Rev. Lett. **98**, 051801 (2007); K.-F. Chen *et al.* (Belle Collaboration), Phys. Rev. Lett. **94**, 221804 (2005).
[5] A. Kagan, Phys. Lett. B **601**, 151 (2004); C. Bauer *et al.*, Phys. Rev. D **70**, 054015 (2004); P. Colangelo *et al.*, Phys. Lett. B **597**, 291 (2004); M. Ladisa *et al.*, Phys. Rev. D **70**, 114025 (2004); H.-n. Li and S. Mishima, Phys. Rev. D **71**, 054025 (2005); M. Beneke *et al.*, Phys. Rev. Lett. **96**, 141801 (2006).
[6] A. Datta *et al.*, Phys. Rev. D **76**, 034015 (2007).
[7] D. Atwood and A. Soni, Phys. Rev. D **65**, 073018 (2002).
[8] A. Ali, G. Kramer, and C.-D. Lu, Phys. Rev. D **58**, 094009 (1998); L. Chau *et al.*, Phys. Rev. D **45**, 3143 (1992); H.-Y. Cheng and K.-C. Yang, Phys. Lett. B **511**, 40 (2001); W. Zou and Z. Xiao, Phys. Rev. D **72**, 094026 (2005).
[9] M. Beneke, J. Rohrer, and D. Yang, Nucl. Phys. **B774**, 64 (2007).
[10] R. Godang *et al.* (CLEO Collaboration), Phys. Rev. Lett. **88**, 021802 (2001).
[11] B. Aubert *et al.* (*BABAR* Collaboration), Nucl. Instrum. Methods Phys. Res., Sect. A **479**, 1 (2002).
[12] G. Kramer and W. F. Palmer, Phys. Rev. D **45**, 193 (1992).
[13] S. Brandt *et al.*, Phys. Lett. **12**, 57 (1964); E. Fahri, Phys. Rev. Lett. **39**, 1587 (1977).
[14] B. Aubert *et al.* (*BABAR* Collaboration), Phys. Rev. D **70**, 032006 (2004).
[15] B. Aubert *et al.* (*BABAR* Collaboration), Phys. Rev. Lett. **89**, 201802 (2002).
[16] H. Albrecht *et al.* (ARGUS Collaboration), Phys. Lett. B **241**, 278 (1990).
[17] D. Aston *et al.* (LASS Collaboration), Nucl. Phys. **B296**, 493 (1988).